

LNF - 70/36  
22 Luglio 1970

B. Bartoli, B. Coluzzi, F. Felicetti, G. Goggi, G. Marini, F. Ma  
sa, D. Scannicchio, V. Silvestrini and F. Vanoli: ELECTRON-  
POSITRON ELASTIC SCATTERING AT HIGH ENERGIES.

Nota Interna: n. 487  
22 Luglio 1970

B. Bartoli, B. Coluzzi, F. Felicetti, G. Goggi<sup>(x)</sup>, G. Marini<sup>(o)</sup>, F. Massa<sup>(x)</sup>,  
D. Scannicchio<sup>(x)</sup>, V. Silvestrini and F. Vanoli<sup>(x)</sup>: ELECTRON-POSITRON  
ELASTIC SCATTERING AT HIGH ENERGIES. -

(Submitted to the Kiev International Conference on High Energy Physics,  
August, 1970).

In an experiment to search for the possible production of new  $J^{PC} = 1^{--}$  neutral bosons in  $e^+e^-$  interactions at ADONE, the Frascati  $2 \times 1.5$  GeV  $e^+e^-$  storage ring<sup>(1)</sup>, approximately 1700  $e^+e^-$  wide angle elastic scattering events were collected in addition to the hadronic events discussed in another paper<sup>(2)</sup>. In the runs performed up to now the energy of the incident electrons and positrons was fixed at several different values between 0.8 and 1.0 GeV.

- 
- (x) - Istituto di Fisica dell'Università di Pavia; Istituto Nazionale di Fisica Nucleare - Gruppo di Pavia, Italy.
  - (o) - Istituto di Fisica dell'Università di Roma; Istituto Nazionale di Fisica Nucleare - Sezione di Roma, Italy.
  - (x) - Istituto di Fisica Superiore dell'Università di Napoli; Istituto Nazionale di Fisica Nucleare - Sezione di Napoli, Italy.

2.

Comparing the observed wide angle  $e^+e^-$  elastic scattering rate with the "monitor", i. e. the rate of  $e^+e^-$  small angle scattering events measured in a separate apparatus<sup>(3)</sup>, a test of the validity of quantum electrodynamics (QED) is obtained with squared space-like momentum transfers to the virtual photon up to  $\sim 1.7$  (GeV/c)<sup>2</sup>. The experimental results are in agreement with theory.

Schematic views of the experimental apparatus are shown in Fig. 1. Four identical telescopes ( $T_1, \dots, T_4$ ) surrounding one of the experimental straight sections of ADONE, cover about 0.35 of the total solid angle. Each telescope,  $T_i$ , consists of:

- four counters  $A_i, B_i, C_i, D_i$  (plastic scintillators);
- two magnetostrictive monogap wire spark chambers  $\alpha_i$  and  $\beta_i$ , in which the azimuthal direction (z-axis along the beam direction) of the emitted particles is measured;
- the following absorbers: 1 cm Al between counters  $A_i$  and  $B_i$ , and 0.7 cm Pb between  $B_i$  and  $C_i$  and between  $C_i$  and  $D_i$ .

A thick absorber (22 cm Fe) and a roof of veto counters,  $CR_1$  and  $CR_2$ , above the apparatus give a reduction of a factor  $\sim 100$  in the counting rate due to cosmic rays, while particles coming from reactions which are the object of our study have only a small probability of emerging from the Fe absorber.

A charged particle in the telescope  $T_i$  is defined by the coincidence

$$T_i \equiv A_i B_i (C_i + D_i)$$

while a neutral particle,  $N_i$ , is defined as  $N_i \equiv (\bar{A}_i + \bar{B}_i)(C_i + D_i)$ . The master coincidence,  $M$ , is defined by any coincidence of order  $\geq 2$  among the  $T_i$ 's, with  $CR \equiv (CR_1 + CR_2)$  in anticoincidence.

When a master  $M$  occurs, the spark chambers are triggered, and the following information is recorded with a small on-line PDP-8 computer:

- i) the coincidences  $T_i$ 's involved in the master;
- ii) the time separation,  $\Delta t$ , between the occurrence of the event and a reference time fixed with respect to the phase of the radio-frequency (R.F.) accelerating voltage of the storage ring<sup>(4)</sup>;
- iii) four pulse heights  $H_i$ , each  $H_i$  being the sum of the pulse heights in counters  $C_i$  and  $D_i$ ;
- iv) the transverse coordinate (orthogonal to the beam) of any event in each of the spark chambers  $\alpha_i, \beta_i$ , with the restriction, however, that if there is more than one track in the same chamber, we read only the coordinate of the track closest to the magnetostrictive pick-up.

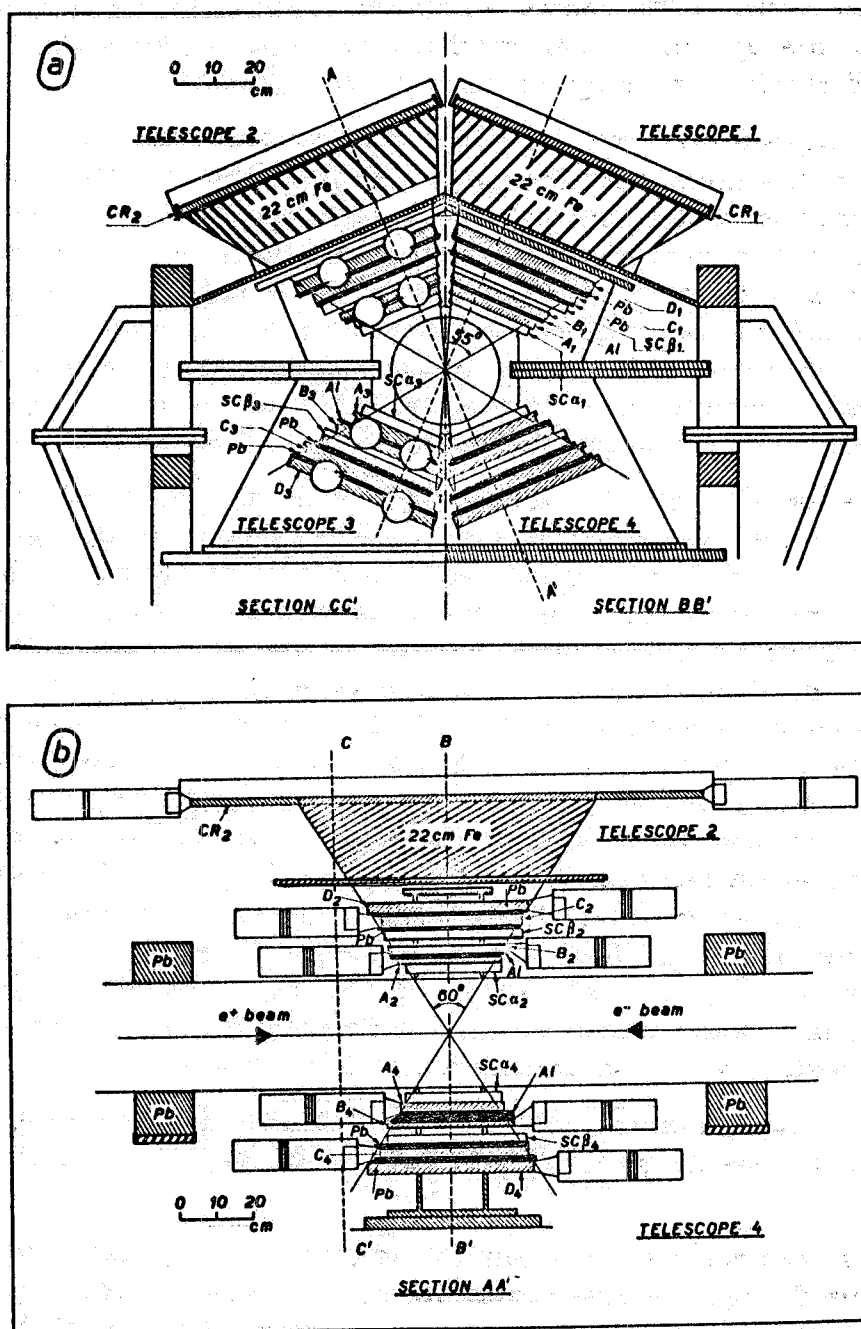


FIG. 1 - The experimental apparatus. - a) Section orthogonal to the beam axis:  $A_i$ ,  $B_i$ ,  $C_i$ ,  $D_i$  are plastic scintillator counters;  $SC\alpha_i$  and  $SC\beta_i$ , magnetostriuctive monogap wire chambers;  $CR_1$  and  $CR_2$ , the veto counters for cosmic rays. b) Section in a plane through the beam direction and orthogonal to a pair of opposite telescopes.

This information is recorded, event by event, on magnetic tape for later analysis at the 1108 Univac computer of the University of Rome. During each run histograms of uncorrelated spectra for each telescope are accumulated in a live display for monitoring purposes.

In the analysis we first classify the events as "in-phase" and "out-of-phase" with the beam-beam impact. The distribution of the number of events as a function of  $\Delta t$ , shows a peak superimposed on a flat background due to cosmic rays; the peak corresponds to the time distribution of the overlap of the colliding bunches folded with our experimental time resolution. This allows us to define the time distance  $\Delta \tau$  between the occurrence of each event and the center of the collision distribution. We define as "in-phase" events (p. e.) the ones which occur within the collision time interval, as "out-of-phase" events (o. p. e.) the outside ones.

The  $e^+e^- \rightarrow e^+e^-$  elastic scattering events are to be selected among the p. e., in the coincidences between two opposite telescopes ( $T_1 T_3$  or  $T_2 T_4$ ). The selection is based on the analysis of the pulse heights  $H_i$ 's in the telescopes involved, since the electrons have a high probability ( $\geq 90\%$ ) of producing a detectable shower in the lead-scintillator sandwiches  $C_i, D_i$ . Typical plots of  $H_1$  vs  $H_3$  are shown in Fig. 2a, 2b. In figure 2a, only "in-phase" events (p. e. for which  $|\Delta \tau| \leq 4$  nsec) are plotted; Fig. 2b shows the plot of the o. p. e. ( $|\Delta \tau| > 4$  nsec). If we set arbitrary upper and lower boundaries  $H_{i, \max}$  and  $H_{i, \min}$  for minimum ionizing particles (" $\mu$ ") crossing the telescope  $T_i$ , we can divide the plane of Fig. 2 into four different regions above  $H_{i, \min}$  and  $H_{j, \min}$ . (The boundaries are selected so that  $\sim 99\%$  of the minimum ionizing particles occur between  $H_{i, \min}$  and  $H_{i, \max}$ .) It can be seen that the large pulse heights region ("e-e"), which is practically empty in Fig. 2b, is fairly heavily populated in Fig. 2a. Those events in which both particles give rise to a shower ("e-e" events), are good candidates as  $e^+e^-$  events.

Actually, the additional information available allows one to conclude that the "e-e" events are, almost without exception, elastic scattering events.

Fig. 3a shows the distributions of the distance,  $L_i$ , between the track in telescope  $T_i$  and the axis of the beam, for "e-e" events.  $L_i$  is positive or negative according to the relative position of the particle trajectory in respect to the beam line. From Fig. 3a it appears that all the events originate in the beam region within  $\pm 7.5$  mm. The actual transverse dimensions of the beam are  $\sim 1 \times 1$  mm<sup>2</sup>, but multiple scattering in the vacuum chamber walls and in the absorbers of the telescopes accounts for the observed width.

Fig. 3b shows the distribution of the angle  $\Delta \phi$  between the two planes parallel to the beam axis and containing the two tracks of the "e-e" events: the events appear to be coplanar within  $\pm 3^\circ$  (h. w. h. m.). Such a

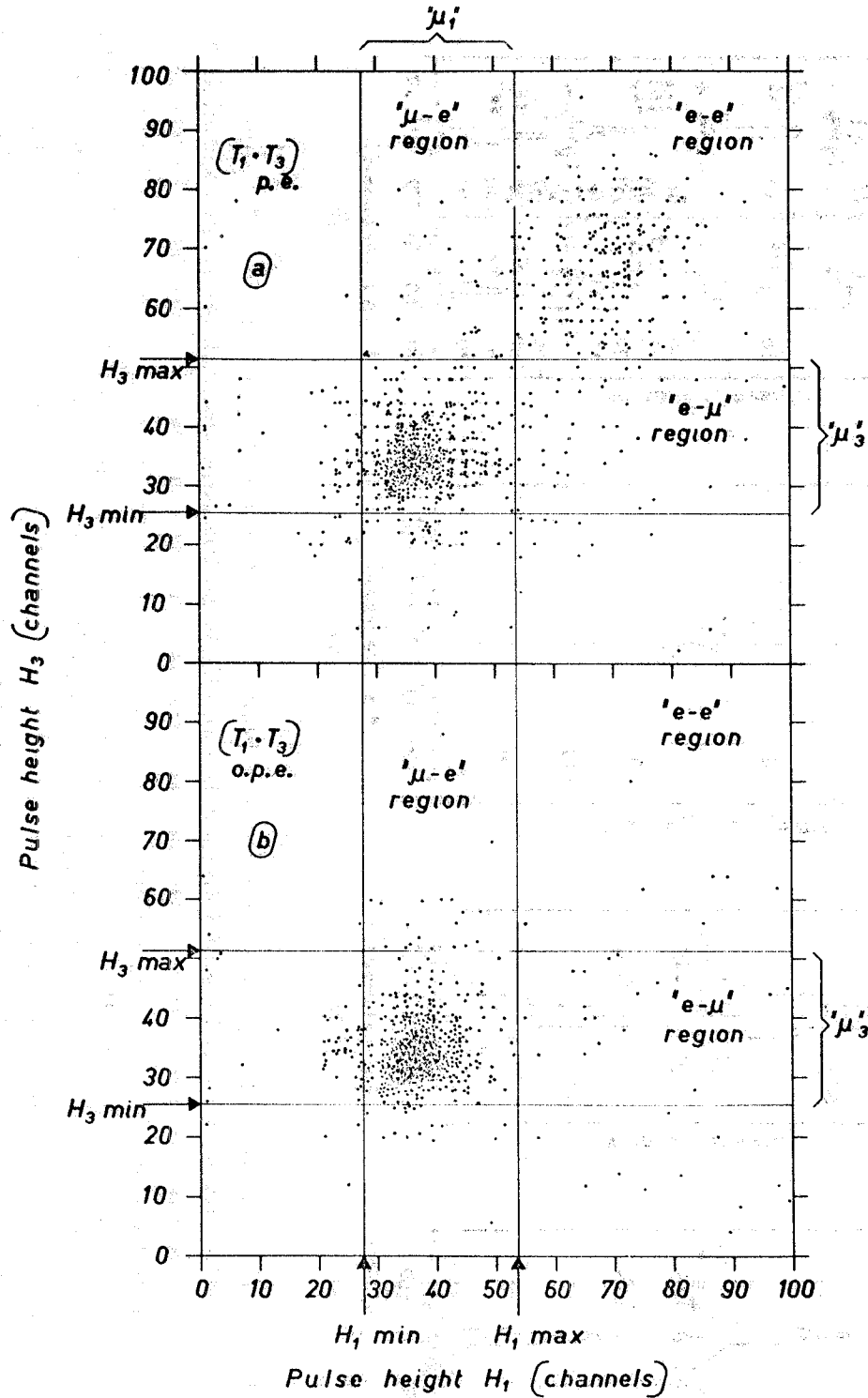


FIG. 2 - Pulse height analysis of  $(T_1 \cdot T_3)$  events. -  
 a) Plot of  $H_3$  vs  $H_1$  pulse heights, for  $(T_1 \cdot T_3)$  events which are "in-phase" with the bunches (p. e.,  $|\Delta\tau| \leq 4$  nsec). The "e-e", " $\mu$ -e", "e- $\mu$ " regions contain candidates for  $e^+e^- \rightarrow e^+e^-$  events (see text). From now on events in both " $\mu$ -e" and "e- $\mu$ " regions will be called " $\mu$ -e" events.  
 b) The same as a), but referred to "out-of-phase" events (o. p. e.,  $|\Delta\tau| > 4$  nsec).

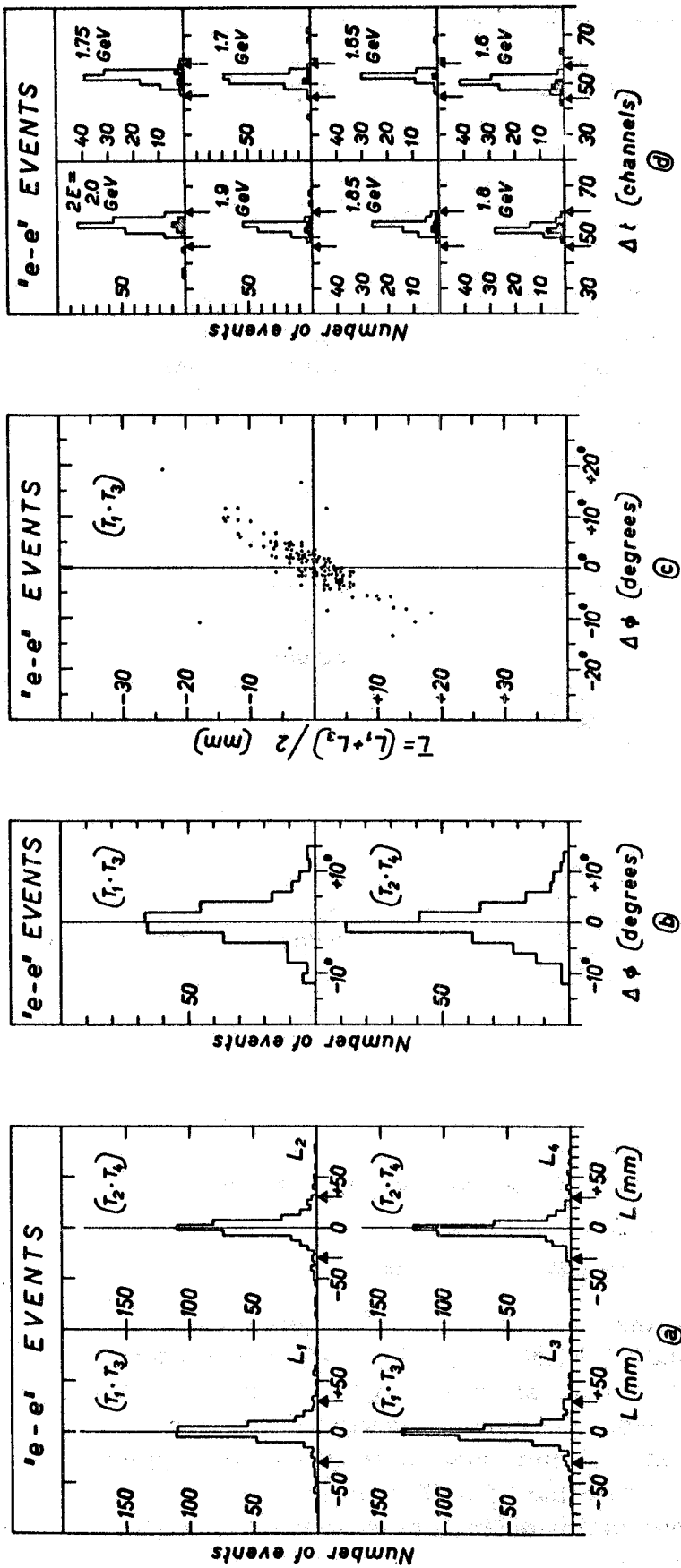


FIG. 3 - Track analysis and time distributions of the "e-e" events. - a) The number of the "e-e" events as a function of the distance,  $L_i$ , between the line of flight of the particle in the telescope  $T_i$  and the axis of the beam (positive  $L_i$  particles come from one side of the beam, negative ones from the other side). b) "e-e" events distribution as a function of  $\Delta\phi$ , the angle between the two planes parallel to the beam axis and containing the two different tracks associated with each "e-e" event. c)  $\bar{L}$  vs  $\Delta\phi$  plot for  $(T_1 \cdot T_3)$  "e-e" events. d) Time distributions of "e-e" events for several different values of the C. M. total energy  $2E = E_+ + E_-$ .  $\Delta t$  is the time separation between the occurrence of the event and a reference time fixed with respect to the phase of the radio frequency (R. F.) accelerating voltage of the storage ring (1 channel  $\approx 0.7$  nsec). The arrows define the beam-beam collision intervals, slightly different at different energies  $2E$ .

spread is expected from multiple scattering in the telescopes and this interpretation is confirmed by the results shown in Fig. 3c. In this figure we have plotted the angle  $\Delta\phi$  for each event against  $\bar{L}$ , the mean of  $L_1$  and  $L_3$  or  $L_2$  and  $L_4$ . The correlation between  $\Delta\phi$  and  $\bar{L}$  is clearly seen.

The  $\Delta t$  distribution for "e-e" events (Fig. 3d) confirms that the contamination from the o. p. e. is negligible.

Finally, background measurements performed with only a single beam ( $e^-$ ) in the machine, allow us to evaluate the contamination from interactions of electrons with the residual gas as  $(2.1 \pm 0.7)\%$ (5).

We thus conclude that the "e-e" events, after the small background subtraction ( $\sim 2\%$ ), are two body events with charged light electromagnetic particles from  $e^+e^-$  collisions, and are, therefore,  $e^+e^- \rightarrow e^+e^-$  elastic scattering events.

The track analysis made above required that all of the four spark chambers involved in each event showed a track. However, since the efficiency of each chamber has been measured to be 0.85 to 0.90, we would lose in this way a large number of  $e^+e^- \rightarrow e^+e^-$  events. As the track analysis demonstrates all the "e-e" events to be  $e^+e^- \rightarrow e^+e^-$ , we use, for the evaluation of the cross section all the events satisfying the pulse height requirements, avoiding in this way problems connected with spark chamber efficiency.

Since the probability that an electron will initiate a shower, before getting through the counters  $C_i + D_i$ , is less than 100%, we expect that a fraction of the events  $e^+e^- \rightarrow e^+e^-$  will appear in the form of events marked as " $\mu$ -e" in Fig. 2a. To evaluate this correction, the " $\mu$ -e" events have also been analyzed in the same manner as the "e-e" events.

The  $|\Delta\phi|$  distribution for the p. e. " $\mu$ -e" events ( $|\Delta\tau| \leq 4$  nsec) is shown in Fig. 4a. There is a substantial peak of coplanar events. The  $L$  distribution for these coplanar events ( $|\Delta\phi| \leq 10^\circ$ ) is shown in Fig. 4b; again we see that the majority of them comes from the source. By appropriately subtracting the background events (o. p. e.), we are thus able to evaluate the probability  $\epsilon$  for an electron to appear in a " $\mu$ -e" region of Fig. 2a, which turns out to be  $\epsilon = (7.2 \pm .8)\%$ . The total correction to be applied to the "e-e" events is therefore  $(1 - \epsilon)^{-2} = (1.16 \pm .02)$ .

The total number of the "e-e" events collected is given in the fourth column of Table I for different values of the C. M. total energy  $2E = E_+ + E_-$ ; the corresponding numbers of  $e^+e^- \rightarrow e^+e^-$  events, corrected for shower inefficiency and e-gas background, are given in the sixth column ( $e^+e^-$ ).

The corrected number of  $e^+e^- \rightarrow e^+e^-$  events are compared with the "monitor" events,  $m$ , collected at the same time (7th column of



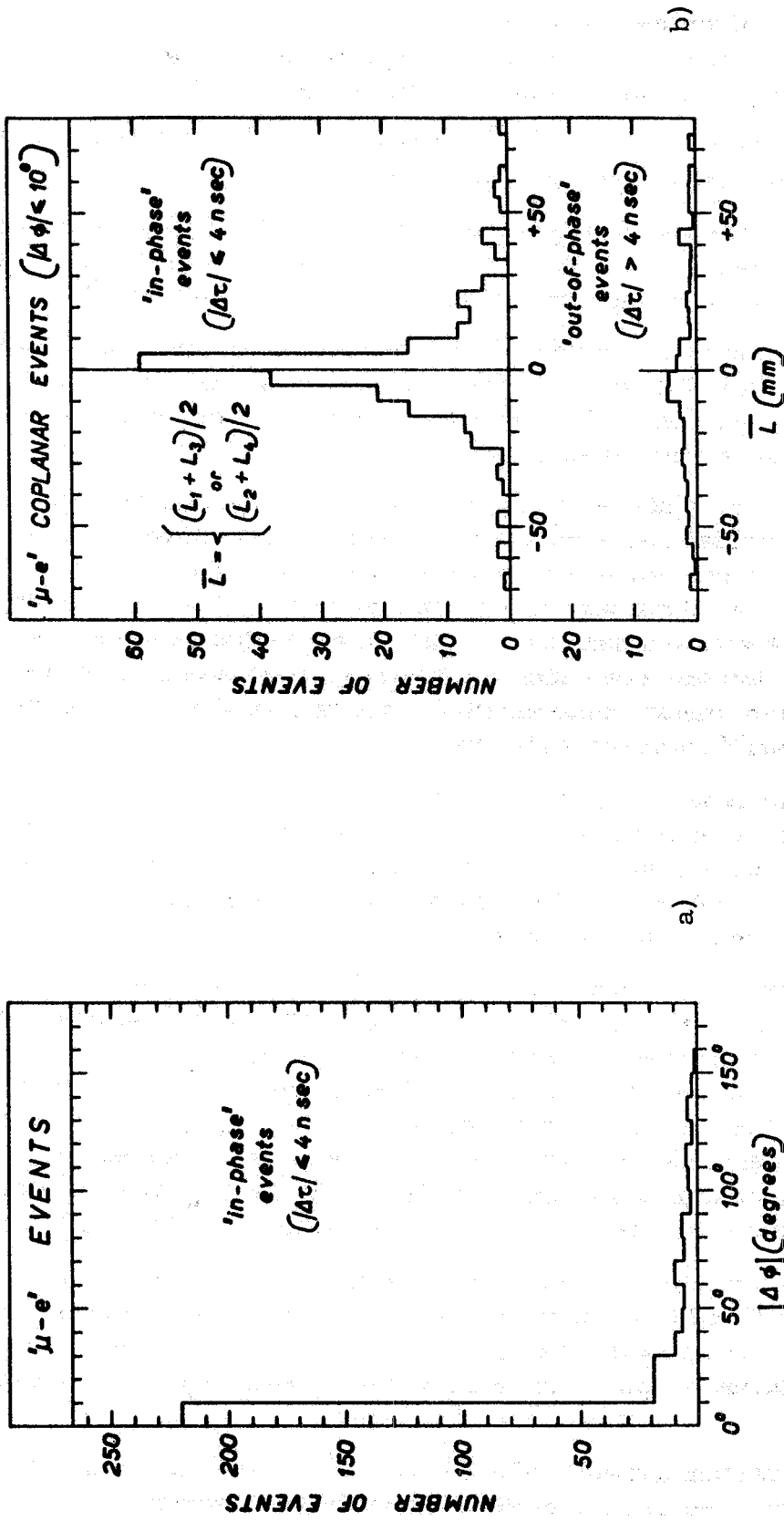


FIG. 4 - Track analysis of the " $\mu$ -e" events. - a)  $|\Delta\phi|$  distribution of the " $\mu$ -e" events which are "in-phase" with the bunches (p. e.,  $|\Delta\tau| \leq 4$  nsec). b) Number of coplanar ( $|\Delta\phi| \leq 10^\circ$ ) " $\mu$ -e" events as a function of  $\bar{L}$  (see caption of Fig. 3). The lower spectrum is obtained from o. p. e. ( $|\Delta\tau| > 4$  nsec) and it is normalized for appropriate cosmic rays background subtraction.

TABLE I

(1) 2E=E <sub>+</sub> +E <sub>-</sub> (MeV)	(2) Total running time (minutes)	(3) Integrated luminosity (cm <sup>-2</sup> )	(4) "e-e" events detected	(5) Normalized e-gas interac- tion background	(6) Wide angle scat- tering events cor- rected for e-gas background and shower inefficiency	(7) Small angle scattering "mo- nitor" events	(8) $R = \frac{e^+e^-}{m}$ (statistical errors)	(9) q <sup>2</sup> (GeV/c) <sup>2</sup>
2000	6833	271 x 10 <sup>32</sup>	331	13.5 ± 4.0	368.3 ± 22.4	125.9 x 10 <sup>3</sup>	2.92 ± .18	1.680
1900	3587	131	183	4.0 ± 1.2	207.6 ± 16.1	70.4	2.95 ± .23	1.516
1850	2725	129	168	2.1 ± 0.6	192.5 ± 15.4	75.6	2.54 ± .20	1.437
1800	4373	133	226	5.5 ± 1.7	255.8 ± 18.1	84.1	3.04 ± .21	1.361
1750	5466	130	182	4.2 ± 1.3	206.2 ± 16.1	88.3	2.34 ± .18	1.286
1700	4873	122	251	3.2 ± 1.0	287.4 ± 19.0	90.5	3.17 ± .21	1.214
1650	4023	98	187	2.4 ± 0.7	214.1 ± 16.3	80.3	2.67 ± .20	1.143
1600	3653	73	171	1.1 ± 0.3	197.2 ± 15.5	64.4	3.06 ± .24	1.075
TOTAL	35533	1087 x 10 <sup>32</sup>	1699	36.0 ± 10.8	1929.1 ± 59.0	679.5 x 10 <sup>3</sup>	2.83 ± .09	

Table I), namely with small angle  $e^+e^- \rightarrow e^+e^-$  elastic scattering events<sup>(3)</sup> ( $3.5^\circ \leq \theta \leq 6^\circ$ ) measured with a separate experimental apparatus on a contiguous straight section of Adone<sup>(6)</sup>. The ratios,  $R$ , of the wide angle scattering to the monitor events are given, with their statistical errors, in the 8th column of Table I.

From QED we can predict the ratio  $R_{th}$  of  $e^+e^-/m$ , by integrating the Bhabha cross-section<sup>(7)</sup> over the experimental apparatus in which the large angle and small angle  $e^+e^-$  scattering events are collected.

However some problems arise from the fact that the source (product of the densities of  $e^+$  and  $e^-$  in the bunches) has a finite longitudinal dimension. The expected distribution is

$$N(\ell) = N_0 \exp(-\ell^2/2\bar{\ell}^2)$$

where  $\bar{\ell}$  is comparable with the linear dimensions of our apparatus.

Theoretically<sup>(8)</sup>,  $\bar{\ell}$  is expected to be  $\bar{\ell} \text{ (cm)} = 20 E_+^{3/2}$  ( $E_+$  in GeV), and experimentally<sup>(8)</sup> has been determined as  $\bar{\ell} = (22 \pm 2) E_+^{3/2}$ . This  $\pm 10\%$  error in  $\bar{\ell}$  corresponds to an error  $\Delta R_{th}/R_{th}$  as small as  $\pm 2\%$ , since the efficiencies of the large angle and the small angle apparatus have approximately the same dependence on  $\bar{\ell}$ .

In evaluating  $R_{th}$ , we have applied the following systematic corrections: losses due to the probability of an electron to be vetoed by the CR counters ( $8 \pm 4\%$ ); multiple scattering losses ( $2.5 \pm 2\%$ ); geometrical misalignment of the experimental apparatus in respect to the beam ( $3 \pm 3\%$ ). Taking also into account a systematic uncertainty in the absolute normalization of the "monitor" ( $\pm 5\%$  as a conservative evaluation), we conclude that the calculated  $R_{th}$  is affected by an overall systematic error of  $\pm 7.5\%$ . Calculated radiative corrections turn out to be negligible ( $\lesssim 1\%$ ).

To compare the experimental results with the calculated  $R_{th}$ , an error  $\pm 5\%$  has to be added to the statistical one associated with each experimental point. This 5% error, is ascribed to some erratic changes in the position of the beam with respect to the "monitor" apparatus, essentially due to variations in the working conditions of the machine in this first period of operation. (This evaluation is based on the comparison between the counting rates of two symmetrical telescopes of the monitor apparatus.)

The experimental results and the corresponding theoretical predictions for  $R_{th}$  are shown in Fig. 5a. The slight dependence of  $R_{th}$  on the total energy  $2E$ , is a consequence of the dependence of  $\bar{\ell}$  on  $E$ . We conclude that in the energy range explored the experimental data show a slope and an absolute value in agreement with the predictions of QED

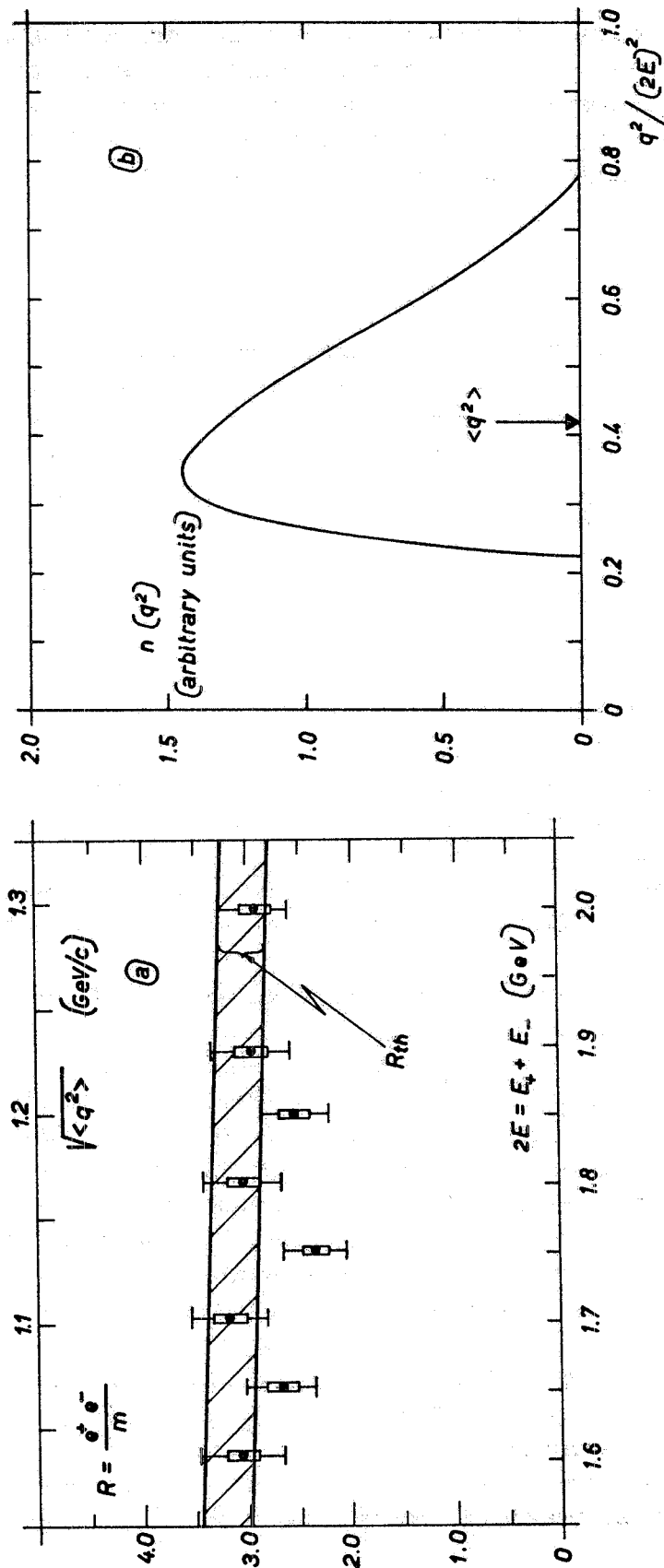


FIG. 5 - a) The ratio,  $R$ , of the  $e^+e^- \rightarrow e^+e^-$  wide angle scattering events detected by our apparatus ( $e^+e^-$ ), to the "monitor" small angle scattering events ( $m$ ), as a function of the C. M. total energy  $2E = E_+ + E_-$ ; experimental results are compared with the theoretical predictions ( $R_{th}$ , see text). In each experimental point, thick lines correspond to the 5% error due to the changes in the beam - "monitor" relative position; thin lines are the statistical errors. b)  $q^2$  acceptance of the experimental apparatus weighted over the Bhabha cross-section, as a function of  $q^2 / (2E)^2$ .  $q$  is the momentum transfer to the virtual space-like photon in the first order scattering diagram;  $\langle q^2 \rangle$ , the average value of the accepted  $q^2$ .

to within the experimental error of  $\sim 10\%$ .

To specify the interval of  $q^2$  we are integrating over, we have plotted in Fig. 5b the spectrum, weighted over the Bhabha cross-section, of the space-like momentum transfer,  $q$ , accepted by our apparatus. The average values,  $\langle q^2 \rangle$ , are also given in the 9th column of Table I, for each C.M. energy  $2E$ , and range between  $\sim 1$  and  $1.7$   $(\text{GeV}/c)^2$ .

We would like to thank Prof. C. Bernardini who participated to the first stage of the experiment; the machine staff for continuous collaboration and discussion; the authors of ref. (3) for having made us available the "monitor" data and all the luminosity informations. We are particularly indebted to our technician G. Schina for his invaluable work on the setting-up and maintenance of the apparatus.

#### REFERENCES AND FOOTNOTES. -

- (1) - F. Amman et al., Status report on the 1.5 GeV electron-positron storage ring Adone, Proc. Intern. Conf. on High Energy Accelerators, Dubna (1963), p. 249.
  - F. Amman et al., Adone the Frascati 1.5 GeV electron-positron storage ring, Proc. V Intern. Conf. on High Energy Accelerators, Frascati (1965), p. 703.
  - F. Amman et al., Adone status report, Proc. Symposium Intern. sur les Anneaux de Collisions, Saclay (1966), III - 2 - 1.
  - F. Amman et al., Two beam operation of the 1.5 GeV electron-positron storage ring Adone, Lettere al Nuovo Cimento, I, 729 (1969).
- (2) - B. Bartoli, B. Coluzzi, F. Felicetti, G. Goggi, G. Marini, F. Massa, D. Scannicchio, V. Silvestrini and F. Vanoli, Multiple particle production from  $e^+e^-$  interactions at C.M. energies between 1.6 and 2 GeV, (PAPER B), sent to the Kiev High Energy International Conference, 1970. Internal Report LNF-70/37, Frascati (1970).
- (3) - G. Barbiellini, B. Borgia, M. Conversi and R. Santonico, A monitoring system to measure the absolute luminosity of the machine Adone operating with  $e^+e^-$  coll. beams, Rendiconti della classe di Scienze Mat. Fis. e Nat. dell'Acc. Naz. dei Lincei, XLIV, 233 (1968).
- (4) - ADONE works with a 3<sup>rd</sup> harmonic R.F. system, so there are three bunches of  $e^+$  and three bunches of  $e^-$  each between 1 and 2 nsec (f. w. h. m.) long; they cross the R.F. cavity when the R.F. phase

equals the synchronous phase  $\bar{\phi}$ , which is slightly dependent on the machine energy, and collide each other in the experimental sections every  $\sim 100$  nsec.

- (5) - This correction has been discussed at greater length in our paper (2) on multiple particle production from  $e^+e^-$  interactions, where this kind of contamination is more severe. The actual value of the normalization factor (to be applied, for appropriate subtraction, to the e-gas interactions events detected in the one beam background runs) has been obtained by comparing, after subtracting cosmic rays events, the counting rates of the T's telescopes. Indeed these rates are directly associated with the interactions of the beam with the residual gas in the machine.
- (6) - The symmetry of the machine and the fact that the data were collected during a long period of time, averaging over possible slight changing of the working condition of the machine, make it reasonable to assume the overall results to be unaffected by the fact that small and large angle elastic scattering were measured in different straight section of Adone.
- (7) - See, for instance; A. I. Akhiezer and V. Beresteski, Quantum Electrodynamics' Interscience, New York (1965), p. 502.
- (8) - Private communications from ADONE machine staff.